NASA Technical Memorandum 89879

Effect of Abrasive Grit Size on Wear of Manganese-Zinc Ferrite Under Three-Body Abrasion

Kazuhisa Miyoshi
Lewis Research Center
Cleveland, Ohio

Prepared for the
1987 Joint Tribology Conference
cosponsored by the American Society of Lubrication Engineers
and the American Society of Mechanical Engineers
San Antonio, Texas, October 5–8, 1987

NASA

EFFECT OF ABRASIVE GRIT SIZE ON WEAR OF MANGANESE-ZINC FERRITE UNDER THREE-BODY ABRASION

Kazuhisa Miyoshi*
National Aeronautics and Space Administration
Lewis Research Center
Cleveland, Ohio 44135

ABSTRACT

Wear experiments were conducted using replication electron microscopy and reflection electron diffraction to study abrasion and deformed layers produced in single-crystal Mn-Zn ferrites under three-body abrasion. The abrasion mechanism of Mn-Zn ferrite changes drastically with the size of abrasive grits. With 15-μm (1000-mesh) SiC grits, abrasion of Mn-Zn ferrite is due principally to brittle fracture; while with 4- and 2-μm (4000- and 6000-mesh) SiC grits, abrasion is due to plastic deformation and fracture. Both microcracking and plastic flow produce polycrystalline states on the wear surfaces of single-crystal Mn-Zn ferrites. Coefficient of wear, total thickness of the deformed layers, and surface roughness of the wear surfaces increase markedly with an increase in abrasive grit size. The total thicknesses of the deformed layers are 3 μm for the ferrite abraded by 15-μm SiC, 0.9 μm for the ferrite abraded by 4-μm SiC, and 0.8 μm for the ferrite abraded by 2-μm SiC.

E-3559

INTRODUCTION

Magnetic heads for telemetry, instrumentation, audio, video, and data recording applications are commonly made of ceramic materials (e.g., Mn-Zn ferrite, Ni-Zn ferrite, and 70Al_2O_3-30TiC). The Mn-Zn ferrite used for this study is generally considered to be highly resistant to abrasive wear,

---

*Member, ASLE.

and this property is a major reason for the selection of this material for magnetic head applications (1-3).

Conventional magnetic recording is accomplished by the relative motion of magnetic media (tape, floppy disks, and rigid disks) against a stationary (audio or computer) or rotating (video) read-write magnetic head. There is physical contact between the media and the head during starting and stopping, or over the entire operating process. This physical contact results in media and head wear and generates wear debris. Head wear is of concern not only because of the cost and inconvenience of replacing heads, but also because of the gradual change in the magnetic characteristics of the head that accompanies the wear process.

Most magnetic media (e.g., magnetic tapes) are inherently abrasive and cause primarily two-body abrasion in magnetic heads (4),(5). In addition, the wear debris particles from the magnetic media and head or the dirt entrained in operating systems can cause media and head wear by three-body abrasion during the operating process.

In the past three symposia the author and his colleagues have published articles concerned with the mechanisms of friction and wear of both the head and the storage media under conditions where two-body abrasion dominates (4), (6-9). This paper, however, concentrates on the study of the abrasive wear of single-crystal Mn-Zn ferrite under conditions where three-body abrasion dominates. Three-body abrasion is the mechanism involved in the finishing of solid surfaces (10-15). For example, the polishing of Mn-Zn ferrite surfaces involves three-body abrasion. The knowledge gained in this study may assist in achieving a better understanding of the characteristics of Mn-Zn ferrite in such operations as polishing.

Therefore, the objective of this paper is to investigate the wear and the deformed layer of single-crystal Mn-Zn ferrite under three-body abrasion and to examine the effect of abrasive grit size on the wear of the ferrite and on the formation of the deformed layer.

MATERIALS

Table 1 presents the composition and hardness data for single-crystal Mn-Zn ferrite {100} surfaces. The as-grown single-crystal Mn-Zn ferrite used in these experiments was better than 99.9 percent pure. The crystallographic orientations of the single-crystal ferrites were determined by the back-reflection Laue method and are to an accuracy of ±1° for the {100} surface.

The single-crystal Mn-Zn ferrite surface was examined by Auger electron spectroscopy (16). The crystal was in the as-polished state. After baking out in a vacuum, the crystal surface was sputter cleaned with argon ions. The Auger spectra revealed that there were small amounts of manganese and zinc on the ferrite surface as well as oxygen and iron in the crystal. The impurities in the crystals were negligibly small. Thus, the single-crystal Mn-Zn ferrite was a high-purity material.

The abrasive grits used in this investigation were silicon carbide (1000-, 4000-, and 6000-mesh) powders. The viscosity of the commercial olive oil lubricant was 85×10^{-6} m^2/s (85 cS) at 20 °C.

APPARATUS

The apparatus used in this investigation was a polishing machine capable of measuring friction during an abrasive wear experiment. The apparatus contained a 160-mm-diameter disk (lapping plate), a conditioning ring (outer diameter, 72 mm; inner diameter, 44 mm), and an arm. The arrangement is shown schematically in Fig. 1.

The arm was pivoted with ball bearings. The pivots allowed the pin to be dead-weight loaded against the disk. The arm contained two flats assembled normal to the direction of friction application. The end of the arm contained the ferrite pin specimen. Under an applied load, the friction force was sensed by strain gauges.

The disk and ring were made of gray cast iron (tensile strength, 210 MPa or higher; Brinell hardness 174 to 197). The disk was rotated by a variable-speed drive. The conditioning ring contained twelve 2-mm-wide grooves that extended radially 30° apart. The conditioning ring was located near the adjustable roller arm (Fig. 1).

The flatness of the lapping disk was maintained to secure accurate tribological results. The surface contour of the disk was changed from concave to convex by moving the ring inwards or outwards. Between these conditions was a ring position that maintained a flat disk contour. Flatness measurements were made by polishing a specimen that was checked with a surface profilometer and a length-measuring machine to determine the direction and approximate amount to move the ring. This procedure was repeated until the disk was flat.

EXPERIMENTAL PROCEDURE

Before every experiment the disk and ferrite pin specimen were lapped with the same abrasives and operating conditions as were applied in the experiment. This allowed the face of the ferrite pin (apparent contact area, 30 mm^2; width, 5 mm; length, 6 mm) to rest flat against the disk.

Abrasive powder was suspended in a lubricant - olive oil. Commercial olive oil is a suspension liquid commonly used for lapping Mn-Zn ferrite in industry. The mixture of the abrasive powder and the olive oil was allowed to drip into the conditioning ring (Fig. 1). The ring assisted in spreading the

mixture and in maintaining the flatness of the disk during the wear experiment. The ratio of abrasive powder to olive oil was 27 wt %. New mixture was added during the wear experiment to maintain the original abrasive grit size. The amount of the mixture supplied, which depended on abrasive grit size, was varied from 3 to 6 cm^3/min to maintain a sufficient oil-film thickness and disk flatness. The sliding velocity was 0.5 m/s.

After the system shown in Fig. 1 was properly conditioned, the Mn-Zn ferrite pin specimen was brought into contact and loaded. The sliding friction experiment was then begun at an apparent contact pressure that ranged from 1 to 10 N/cm^2. The friction force was continuously monitored during sliding. All experiments were conducted in room-temperature (15 to 30 °C) laboratory air at a relative humidity of 50 to 70 percent.

The wear of the ferrite due to abrasion was determined as follows: before and after each experiment, the heights of the ferrite were measured by a length-measuring machine with an accuracy of ±0.15 μm. Then the volume of material removed was calculated from the apparent contact area and the reduction in the height of the ferrite.

The Mn-Zn ferrite was etched with hydrochloric acid at 50±1 °C. The wear and etched surfaces were examined by transmission electron microscopy and reflection electron diffraction in a microscope operating at 100 kV. The surface roughness of the wear surfaces was examined by a stylus technique (surface profilometry).

The abrasives were examined by transmission electron microscopy to establish the best possible grit size and shape of the abrasive employed in this investigation. The abrasives to be examined were suspended in collodion film. To reinforce the collodion film, a carbon film was vacuum-deposited on

the collodion film and abrasives. The abrasive grit size was obtained by measuring 100 to 150 grits in transmission electron photomicrographs.

RESULTS AND DISCUSSION

Abrasive Grits

Figure 2 presents typical transmission electron photomicrographs of the abrasives (1000-, 4000-, and 6000-mesh SiC). The SiC abrasives have a cubelike shape with many sharp edges. The grit shape is not dependent on the abrasive grit size.

Figure 3 presents grit size distribution of the SiC abrasives: that is, the relative amounts of grits of the various sizes included in the powders. Because the grits were shaped irregularly, two dimensions (the largest diameter and the smallest diameter of each particle) were measured from the transmission electron photomicrographs. The bell-shaped curves reveal a generally strong correlation with the normal distribution. Therefore, they are expressed in terms of the normal density function. The average sizes and standard deviation of the measured values of the abrasive grits are listed in Table 2. The 1000-, 4000-, and 6000-mesh abrasives had average grit sizes of 15, 4, and 2 μm (with narrow tolerances), respectively.

The crystalline shape of the SiC grits, particularly the shape of the grits along their largest diameter, makes them very sharp. Figure 4 presents the angle distribution of cutting edges of the abrasive grits along their largest diameter. The angle distributions for the 1000-, 4000-, and 6000-mesh abrasive grits were nearly the same. A large number of the edges had angles ranging from 90° to 100°.

Abrasive Wear

The abrasive grits used in this investigation (1000-, 4000-, and 6000-mesh SiC) abraded the ferrite surfaces in sliding contact. The wear of

single-crystal Mn-Zn ferrites was linearly proportional to the distance of sliding, regardless of the abrasive grit size. The wear was highly reproducible.

Figure 5 presents replication electron photomicrographs and reflection electron diffraction patterns of wear surfaces of single-crystal Mn-Zn ferrite abraded by 15- and 4-μm (1000- and 4000-mesh) SiC grits under the three-body condition. There are actually two wear modes involved in the abrasive processes. With 15-μm SiC grits, abrasion resulted in brittle-fractured facets on the Mn-Zn ferrite surface because of cleavage and quasi-cleavage. With 4-μm SiC grits, a large number of plastically deformed indentations and grooves were produced on the Mn-Zn ferrite surfaces by indenting, plowing, and microcutting. A very few brittle-fractured facets, depending on applied normal load, were observed on the surface abraded by the 4-μm SiC grits.

Polycrystalline diffraction patterns taken on both of the abraded surfaces of single-crystal Mn-Zn ferrite contained continous arcs extending over nearly a semicircle [Figs. 5(a) and (b)]. For the gross fracture surface of the ferrite generated by 15-μm SiC grits, the arcs are much sharper than those generated by 4-μm SiC grits. The sharp arcs are due to microcrack formation on the Mn-Zn ferrite surface caused by 15-μm SiC grits. Such microcracks subdivide a single-crystal Mn-Zn ferrite crystal into polygonal subgrains. The broad arcs indicate a large extent of plastic deformation present on the abraded surface of single-crystal Mn-Zn ferrite. A highly strained Mn-Zn ferrite surface was produced by 4-μm SiC grits. With 2-μm (6000-mesh) SiC grits, wear surfaces and reflection electron diffraction patterns of Mn-Zn ferrite were very similar to those of the surfaces abraded by 4-μm SiC grits. Thus, the abrasion mechanism of the ferrite oxide ceramic changes drastically with the size of the abrasive grits. With 15-μm SiC

grits, ferrite abrasion is principally due to brittle fracture; while with 4- and 2-μm SiC grits, it is due to plastic deformation and fracture.

Deformed Layer

The abrasive grits generated plastic deformation and microcracks and developed a deformed layer on the ferrite surface in sliding contact, as discussed in the previous section. Reflection electron diffraction patterns with chemical depth profiling were obtained for both the wear and etched surfaces to further investigate the crystalline state of the surficial layer of single-crystal Mn-Zn ferrite. The etching was done with hydrochloric acid at 50±1 °C. The results of abrading ferrite surfaces with 15-, 4-, and 2-μm SiC grits are presented in Figs. 6, 7, and 8, respectively.

Figure 6 shows the electron diffraction patterns obtained from the wear and etched surfaces of a single-crystal ferrite abraded by the 15-μm SiC grits. The wear surface was severely distorted and had polycrystalline states [Fig. 6(a)]. The distortion of the ferrite surface verified by the electron diffraction pattern was due mainly to microcracking. The surfaces of the ferrite etched to depths of 1.2 and 1.8 μm from the wear surface had an enlarged streak spot pattern. This type of pattern is caused by a highly distorted, mosaic single-crystal structure containing a large amount of microcracks. The microcracks in the deformed layer decreased as the depths below the wear surface increased. The surface etched to a depth of 3.2 μm had a relatively sharp spot pattern without streaking [Fig. 6(f)]. The surface etched to a depth of 3.3 μm had Kikuchi lines, which indicate a bulk crystalline structure containing no mechanical stress induced during abrasion [Fig. 6(g)]. No microcracks were observed on the surface etched to a depth of 3.3 μm.

Figure 7 shows the electron diffraction patterns obtained from the wear and etched surfaces of the single-crystal Mn-Zn ferrite abraded by 4-μm SiC grits. The wear surface was severely distorted and had polycrystalline states [Fig. 7(a)]. The distortion of the surface is due mainly to plastic deformation and fracture. The surface of the ferrite etched to depths of 0.36 μm from the wear surface indicated a highly strained, mosaic single-crystal structure. The amount of plastic deformation and fracture in the deformed layer decreased as the depth increased to 0.36, 0.50, and 0.54 μm below the wear surface. The surfaces etched to depths of 0.94 and 1.3 μm had Kikuchi lines, which indicate a bulk single-crystal structure. The structure and depth of the deformed layer of ferrite abraded by 2-μm SiC grits were similar to those of ferrite abraded by 4-μm SiC grits (Figs. 7 and 8).

Figure 9 presents a summary of schematic structures for the deformed layers of the abraded single-crystal Mn-Zn ferrites as a function of etching depth (distance from the wear surface). The thickness of the deformed layers, which was determined with reflection electron diffraction by depth profiling, increased markedly with an increase in grit size.

Coefficient of Wear

With 15-μm SiC grits, the abrasive wear of single-crystal Mn-Zn ferrites increased linearly as a function of applied normal load (the apparent contact pressure at the sliding surface of the ferrite specimen) as shown in Fig. 10. For this figure, the average wear rate was defined as the volume of ferrite removed per unit distance of sliding.

On the other hand, the abrasion of the ferrite with 4-μm SiC grits introduced two regimes [Fig. 10(b)]. The wear increased linearly with the applied load, but the rate of increase (slope) changed near a contact pressure of 4 N/cm^2. With 4-μm SiC grits, the abrasion was due principally to

plastic deformation and fracture. There were a very few brittle-fractured facets [Fig. 5(b)]. The number of the brittle-fractured facets increased greatly at apparent contact pressures above the transition pressure.

With 2-μm SiC grits, abrasion of ferrites was linearly proportional to the applied normal load.

The coefficients of wear are presented as a function of abrasive grit size in Fig. 11. Coefficient of wear was strongly dependent on abrasive grit size; that is, it increased markedly with an increase in grit size. Many investigators have found that abrasive wear increases with an increase in the size of the abrasive grit up to a certain critical value and thereafter is independent of grit size (13). The critical grit size (30- to 150-μm diameter) depends strongly on the abrasive, the material, the experimental conditions, and the experimental parameters (e.g., load, velocity, and environment). The grit size in this study was 15-μm in average diameter or smaller. This is much less than the critical grit size found by many investigators (13). Figure 11 clearly indicates that the larger the grit size, the greater the wear rate.

Figure 12 presents the surface roughness of the wear surfaces for single-crystal Mn-Zn ferrites examined by surface profilometry as a function of abrasive grit size. The surface roughness (R_{max}, maximum height of irregularities) depended significantly on the abrasive grit size. The surface roughness increased with an increase in abrasive grit size. The surface roughness of the ferrites abraded by 15-μm SiC grits was about 10 to 15 times greater than that of the ferrites abraded by 4-μm SiC grits.

CONCLUSIONS

The following conclusions were drawn from wear experiments using electron microscopy and electron diffraction to study single-crystal Mn-Zn ferrites under three-body abrasion.

1. There is a drastic change in the abrasion mechanism of Mn-Zn ferrite depending on the size of abrasive grits. With 15-μm (1000-mesh) SiC grits, abrasion of the ferrite is due principally to brittle fracture; while with the 4- and 2-μm (4000- and 6000-mesh) SiC grits, abrasion is due to plastic deformation and fracture.

2. Considerable microcracking (with 15-μm SiC grits) or plastic flow together with fracture (with 4- and 2-μm SiC grits) drastically changes the crystalline state of ferrite surfaces. Polycrystalline states were produced on the wear surfaces of single-crystal Mn-Zn ferrites abraded by 15-, 4-, and 2-μm SiC grits.

3. Coefficient of wear, total thickness of the deformed layers, and surface roughness of the wear surface are strongly dependent on abrasive grit size. They increase markedly with an increase in abrasive grit size.

4. The total thicknesses of the deformed layers are 3 μm for the ferrite abraded by 15-μm SiC, 0.9 μm for the ferrite abraded by 4-μm SiC, and 0.8 μm for the ferrite abraded by 2-μm SiC.

REFERENCES

1. Rabinowicz, E., "The Tribology of Magnetic Recording Systems - An Overview," Tribology and Mechanics of Magnetic Storage Systems, Vol. 3, ASLE SP-21, ed. by B. Bhushan and N.S. Eiss, Jr., ASLE (1986) pp. 1-7.
2. Klaus, E.E., and Bhushan, B., "Lubricants in Magnetic Media - A Review," Tribology and Mechanics of Magnetic Storage Systems, Vol. 2, ASLE SP-19, ed. by B. Bhushan and N.S. Eiss, Jr., ASLE (1985) pp. 7-15.

3. Hahn, F.W. Jr., "Wear of Recording Heads by Magnetic Tape," Tribology and Mechanics of Magnetic Storage Systems, Vol. 1, ASLE SP-16, ed. by B. Bhushan, D. Bogy, N.S. Eiss Jr., and F.E. Talke, ASLE (1984) pp. 41-48.

4. Miyoshi, K., Buckley, D.H., and Tanaka, K., "Effect of Wear on Structure-Sensitive Magnetic Properties of Ceramic Ferrite in Contact With Magnetic Tape," Tribology and Mechanics of Magnetic Storage Systems, Vol. 2, ASLE SP-19, ed. by B. Bhushan and N.S. Eiss Jr., ASLE (1985) pp. 112-118.

5. Bhushan, B., "Assessment of Accelerated Head-Wear Test Methods and Wear Mechanics," Tribology and Mechanics of Magnetic Storage Systems, Vol. 2, ASLE SP-19, ed. by B. Bhushan and N.S. Eiss Jr., ASLE (1985) pp. 101-111.

6 Miyoshi, K. and Buckley, D.H., "Properties of Ferrites Important to Their Friction and Wear Behavior," Tribology and Mechanics of Magnetic Storage Systems, Vol. 1, ASLE SP-16, ed. by B. Bhushan, D. Bogy, N.S. Eiss Jr., and F.E. Talke, ASLE (1984) pp. 13-20.

7. Miyoshi, K., Buckley, D.H., and Tanaka, K., "Abrasion and Deformed Layer Formation of Manganese-Zinc Ferrite in Sliding Contract With Lapping Tapes," Tribology and Mechanics of Magnetic Storage Systems, Vol. 3, ASLE SP-21, ed. by B. Bhushan and N.E. Eiss Jr., ASLE (1986) pp. 42-49.

8. Miyoshi, K., Buckley, D.H., and Tanaka, K., "Effect of Crystallographical and Geometrical Changes of a Ferrite Head on Magnetic Signals During the Sliding Process With Magnetic Tape," Tribology and Mechanics of Magnetic Storage Systems, Vol. 3, ASLE SP-21, ed. by B. Bhushan and N.E. Eiss Jr., ASLE (1986) pp. 50-56.

9. Czichos, H., Tribology, Elsevier North Holland (1978).

10. Rabinowicz, E., Dunn, L.A., and Russell, P.G., "A Study of Abrasive Wear Under Three-Body Conditions," Wear, 4, 345-355 (1961).

11. Rabinowicz, E., "Abrasive Wear Resistance as a Materials Test," Lubr. Eng., 33, 378-381 (1977).

12. Rabinowicz, E., Friction and Wear of Materials, John Wiley and Sons, (1965).

13. Buckley, D.H., Surface Effects in Adhesion, Friction, Wear, and Lubrication, Elsevier, (1981).

14. Tabor, D., "Wear - A Critical Synoptic View," Wear of Materials 1977, ed. by W.A. Glaeser, K.C. Ludema, and S.K. Rhee, ASME, (1977) pp. 1-11.

15. Miyoshi, K., and Buckley, D.H., "Friction and Wear of Single-Crystal and Polycrystalline Manganese-Zinc Ferrite in Contact With Various Metals," NASA TP-1059, (1977).

TABLE 1. - COMPOSITION AND HARDNESS OF SINGLE-CRYSTAL Mn-Zn FERRITE

Composition, wt %	
Fe_2O_3	71.6
MnO	17.3
ZnO	11.1
Knoop hardness number[a]	
{100} plane, <001> direction	630
{100} plane, <0$\bar{1}$1> direction	560
Vickers hardness number[b]	
{100} plane	630

[a]Knoop hardness measuring load, 3 N.
[b]Vickers hardness measuring load, 0.5 N.

TABLE 2. - ABRASIVE GRIT SIZE

	1000-mesh SiC	4000-mesh SiC	6000-mesh SiC
Average of smallest diameters of grit particles, μm	11.2	3.0	1.8
Average of largest diameters of grit particles, μm	17.9	4.5	2.7
Average grit diameter, μm	14.6	3.8	2.3
Ratio of largest to smallest grit diameter	1.7	1.6	1.7
Standard deviation of smallest grit diameters, μm	0.4	0.4	0.4
Standard deviation of largest grit diameters, μm	0.6	0.7	0.5
Standard deviation of average grit diameters, μm	0.4	0.5	0.3
Standard deviation of ratio of largest to smallest grit diameter	0.1	0.1	0.1

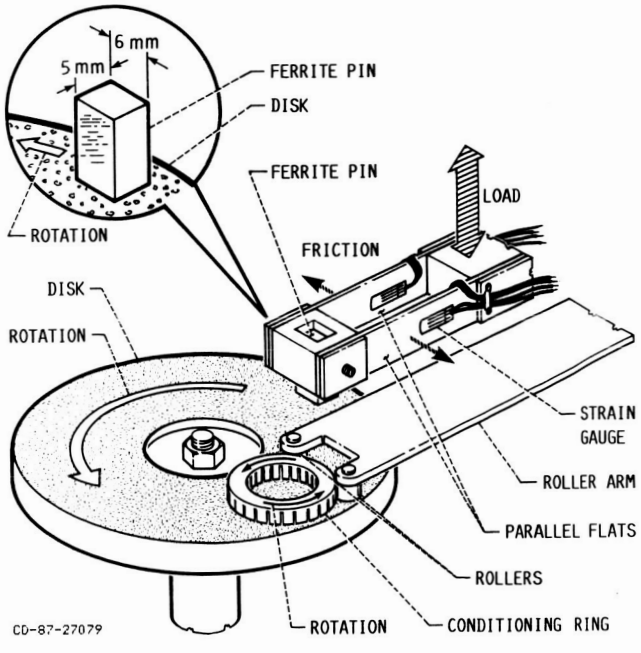

FIGURE 1. - APPARATUS FOR ABRASIVE WEAR.

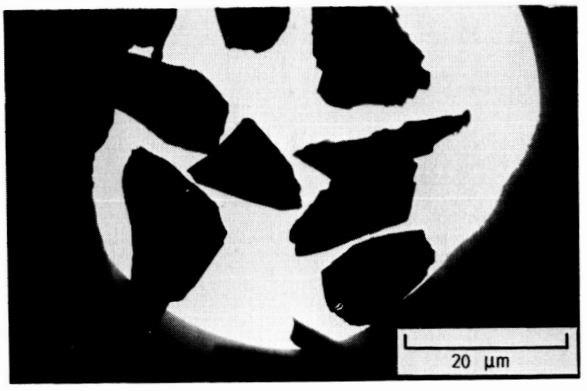

(a) 1000-MESH SiC.

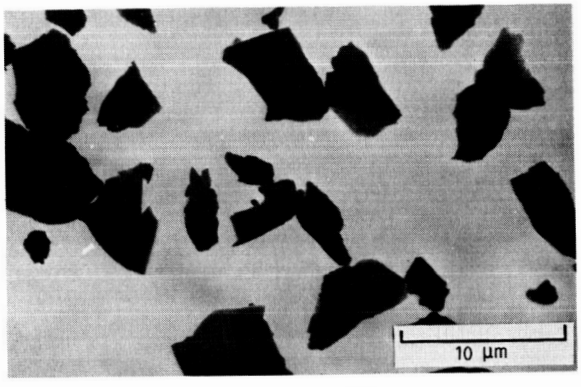

(b) 4000-MESH SiC.

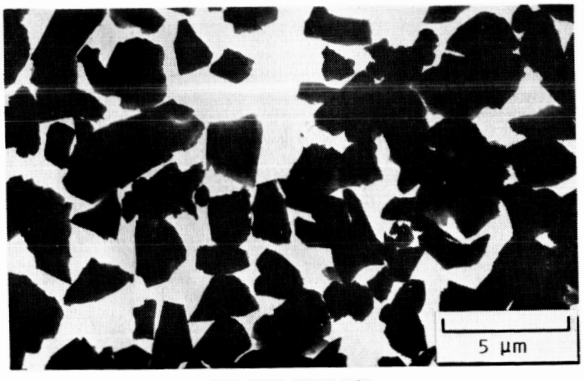

(c) 6000-MESH SiC.

FIGURE 2. - TRANSMISSION ELECTRON PHOTOMICROGRAPHS OF SiC ABRASIVE GRITS.

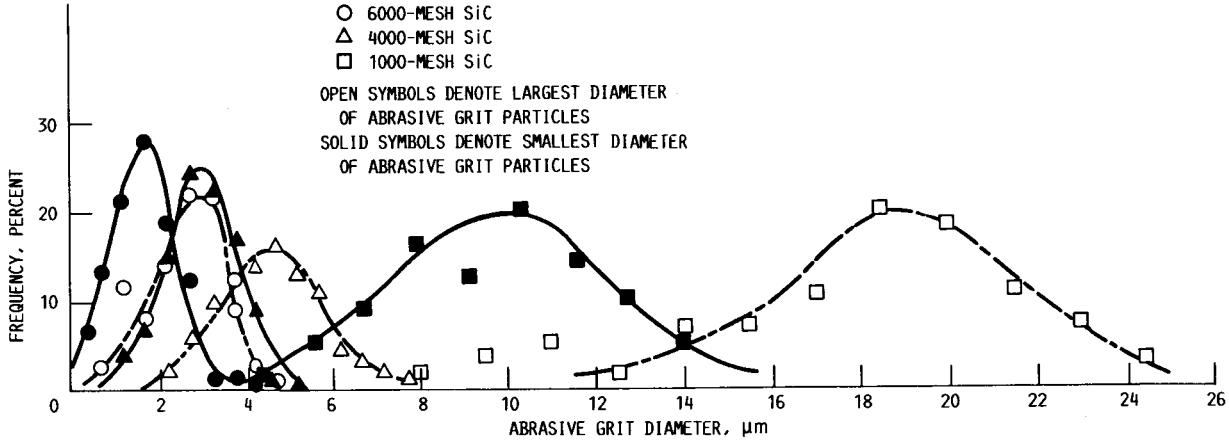

FIGURE 3. - GRIT SIZE DISTRIBUTION OF 1000-, 4000-, AND 6000-MESH SiC ABRASIVES.

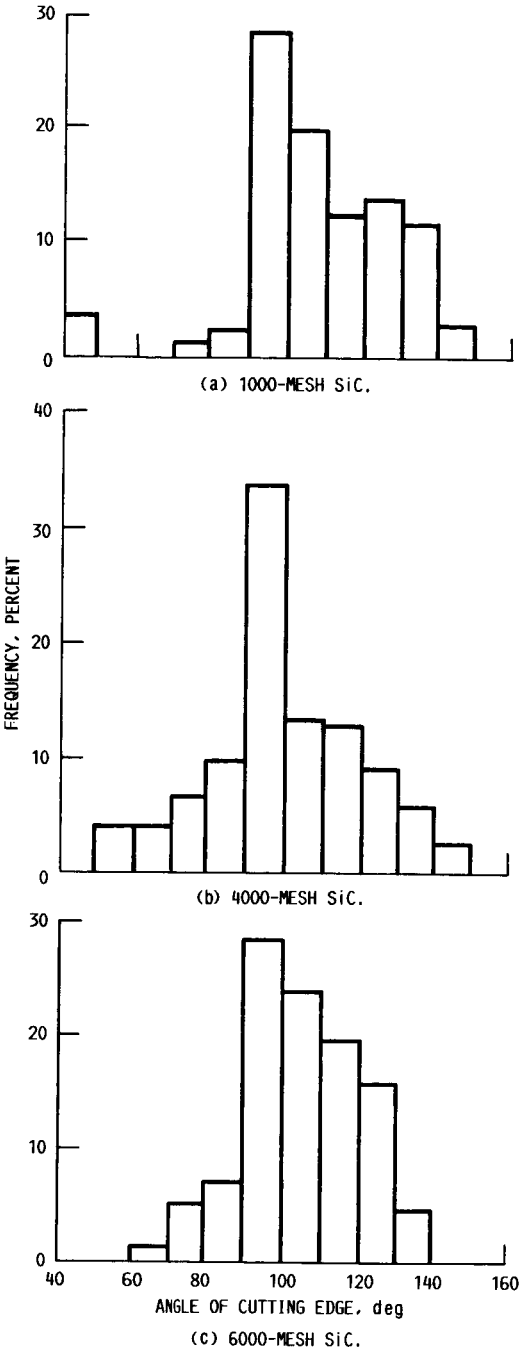

FIGURE 4. - ANGLE DISTRIBUTION OF CUTTING EDGES OF SiC ABRASIVES.

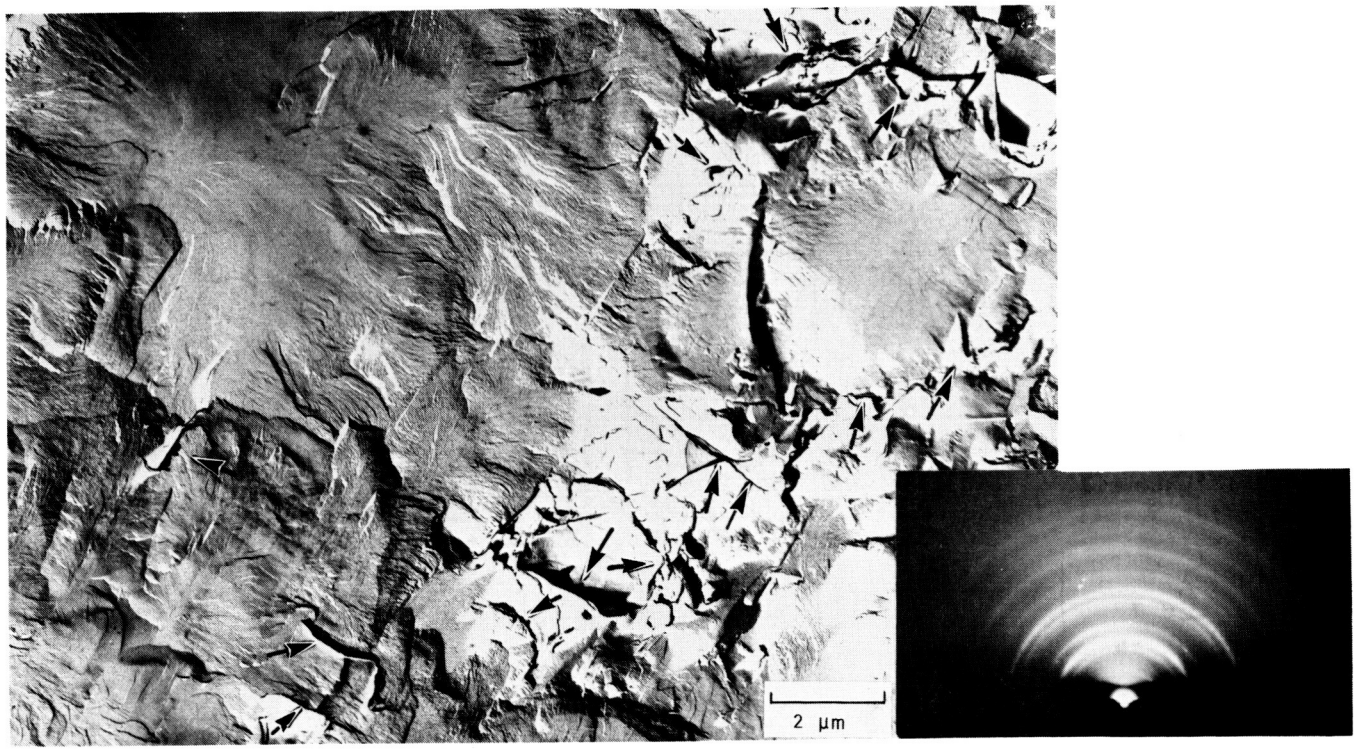

(a) BRITTLE-FRACTURED FACETS GENERATED ON WEAR SURFACE ABRADED BY 15-μm SiC GRITS. APPARENT CONTACT PRESSURE, 3 N/cm^2.

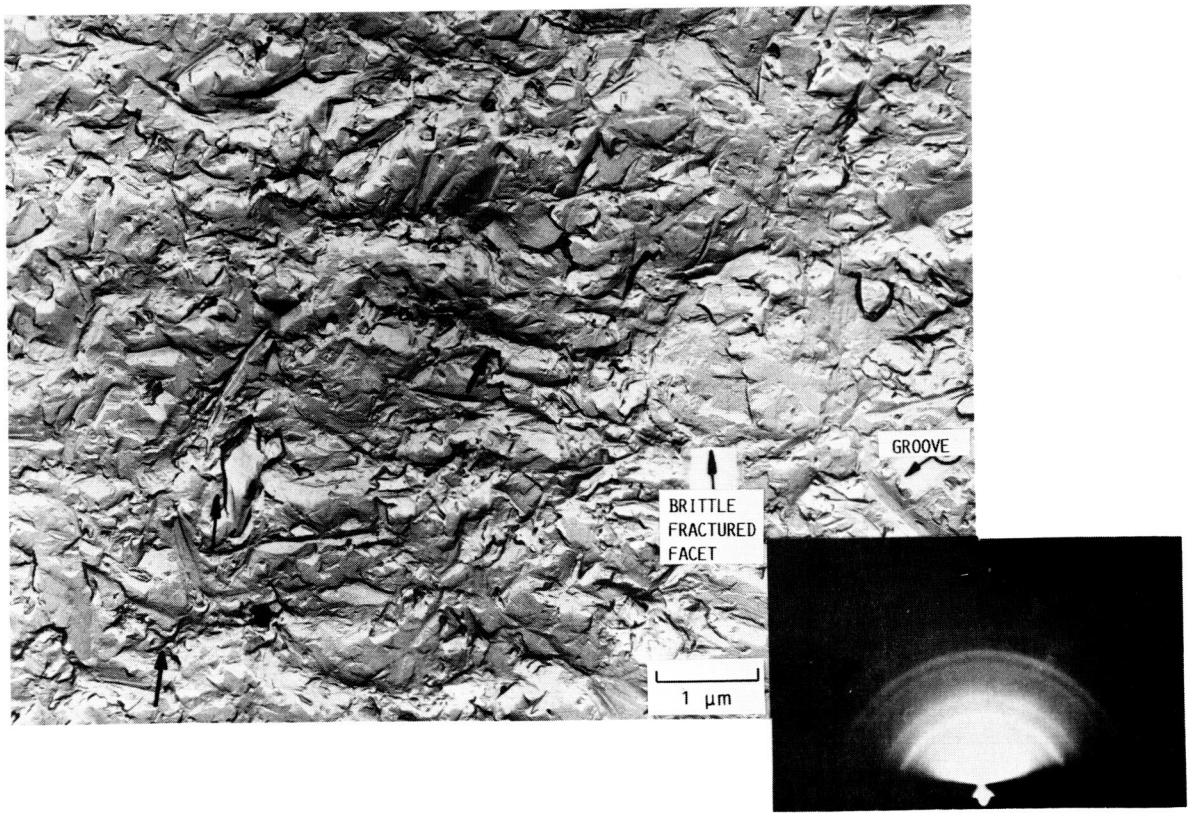

(b) PLASTICALLY DEFORMED INDENTATIONS AND GROOVES GENERATED ON WEAR SURFACE ABRADED BY 4-μm SiC GRITS. APPARENT CONTACT PRESSURE, 8 N/cm^2.

FIGURE 5. - REPLICATION ELECTRON PHOTOMICROGRAPHS AND REFLECTION ELECTRON DIFFRACTION PATTERNS (OPERATING VOLTAGE OF MICROSCOPE, 100 kV) OF ABRADED SURFACES OF CRYSTAL Mn-Zn FERRITES. ARROWS DENOTE CRACKS.

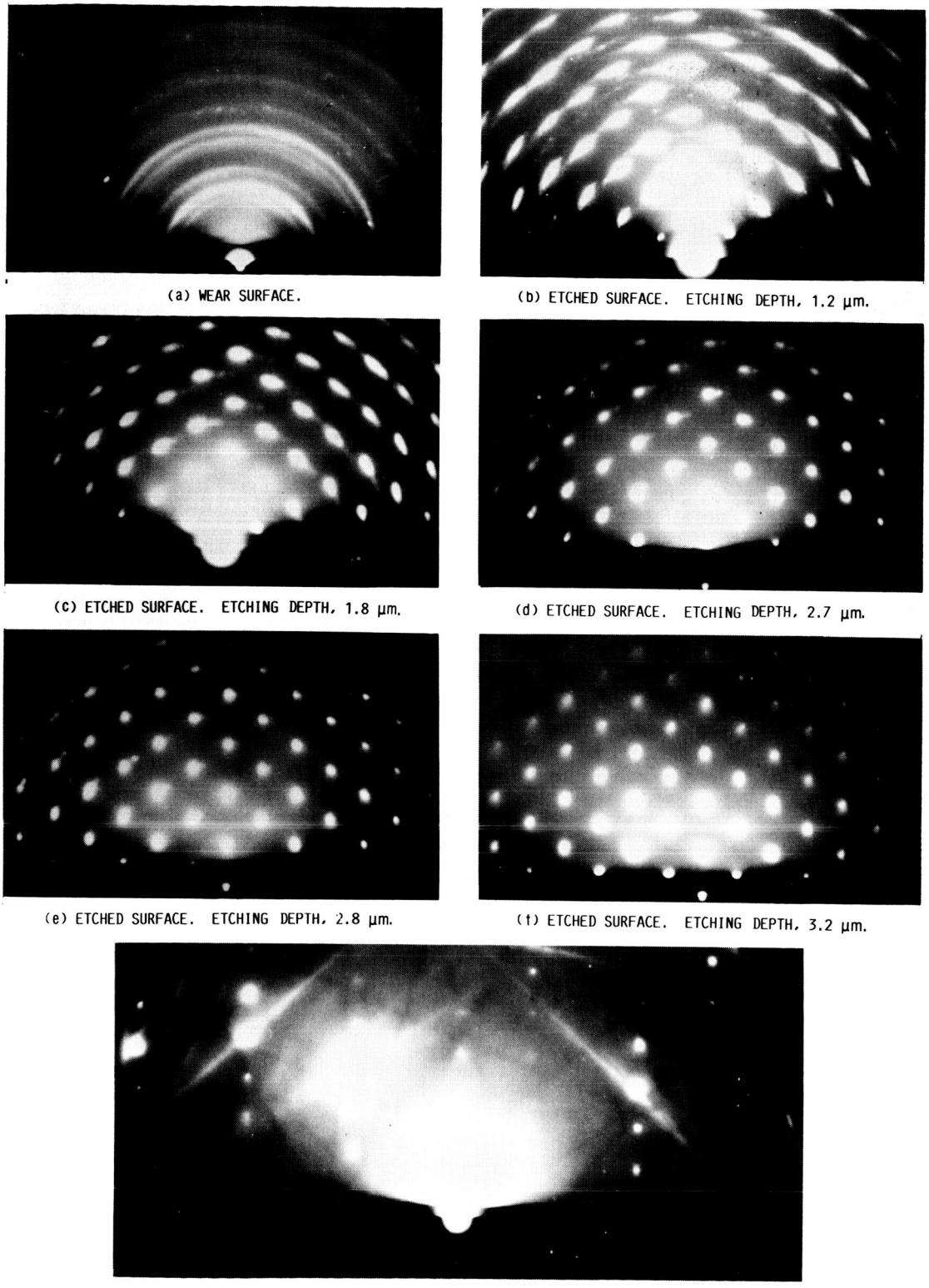

(a) WEAR SURFACE.

(b) ETCHED SURFACE. ETCHING DEPTH, 1.2 μm.

(c) ETCHED SURFACE. ETCHING DEPTH, 1.8 μm.

(d) ETCHED SURFACE. ETCHING DEPTH, 2.7 μm.

(e) ETCHED SURFACE. ETCHING DEPTH, 2.8 μm.

(f) ETCHED SURFACE. ETCHING DEPTH, 3.2 μm.

(g) ETCHED SURFACE. ETCHING DEPTH, 3.3 μm.

FIGURE 6. - DEFORMED LAYER OF SINGLE-CRYSTAL {100} SURFACE OF Mn-Zn FERRITE ABRADED BY 15-μm (1000-MESH) SiC GRITS. APPARENT CONTACT PRESSURE, 4 N/cm^2; SLIDING DIRECTION, <011>.

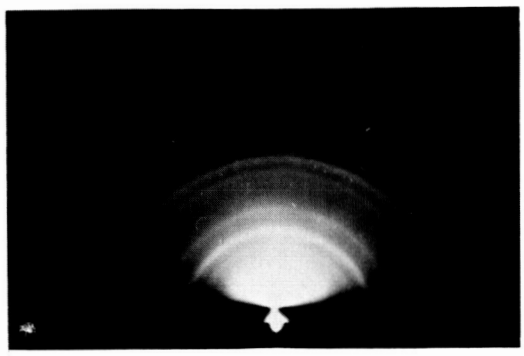

(a) WEAR SURFACE.

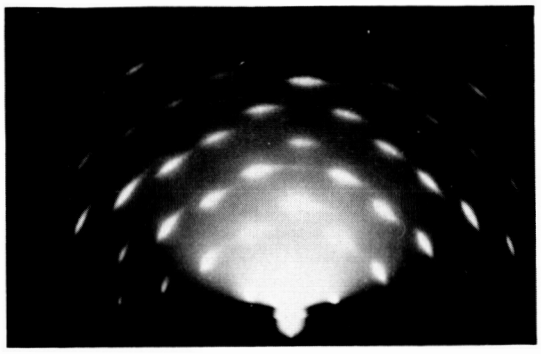

(b) ETCHED SURFACE. ETCHING DEPTH, 0.36 μm.

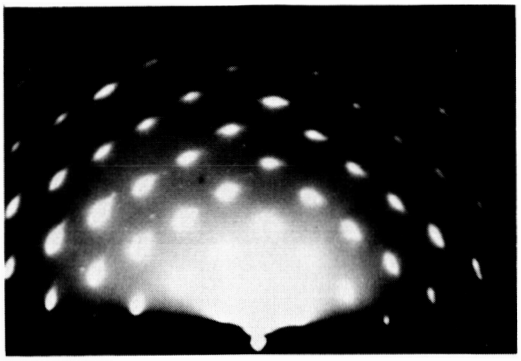

(c) ETCHED SURFACE. ETCHING DEPTH, 0.50 μm.

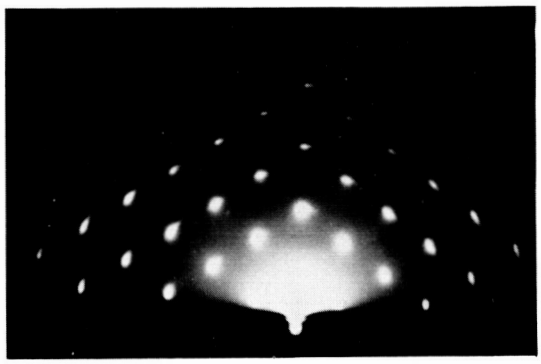

(d) ETCHED SURFACE. ETCHING DEPTH, 0.54 μm.

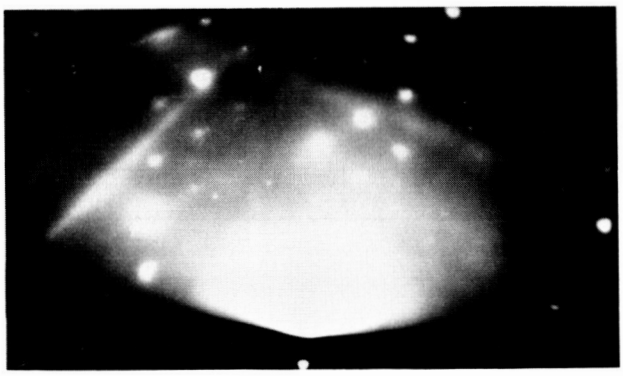

(e) ETCHED SURFACE. ETCHING DEPTH, 0.94 μm.

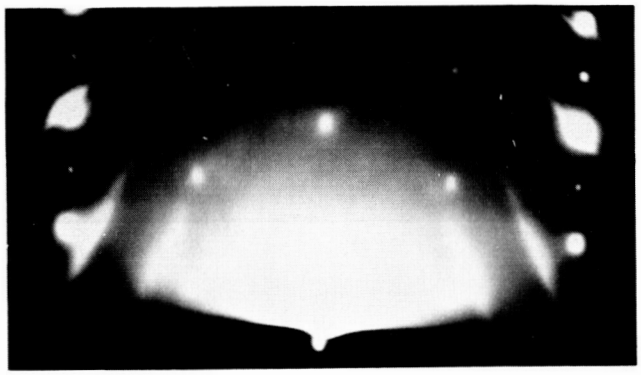

(f) ETCHED SURFACE. ETCHING DEPTH, 1.3 μm.

FIGURE 7. - DEFORMED LAYER OF SINGLE-CRYSTAL {100} SURFACE OF Mn-Zn FERRITE ABRADED BY 4-μm (4000-MESH) SiC GRITS. APPARENT CONTACT PRESSURE, 4 N/cm^2; SLIDING DIRECTION, $\langle 0\bar{1}1 \rangle$.

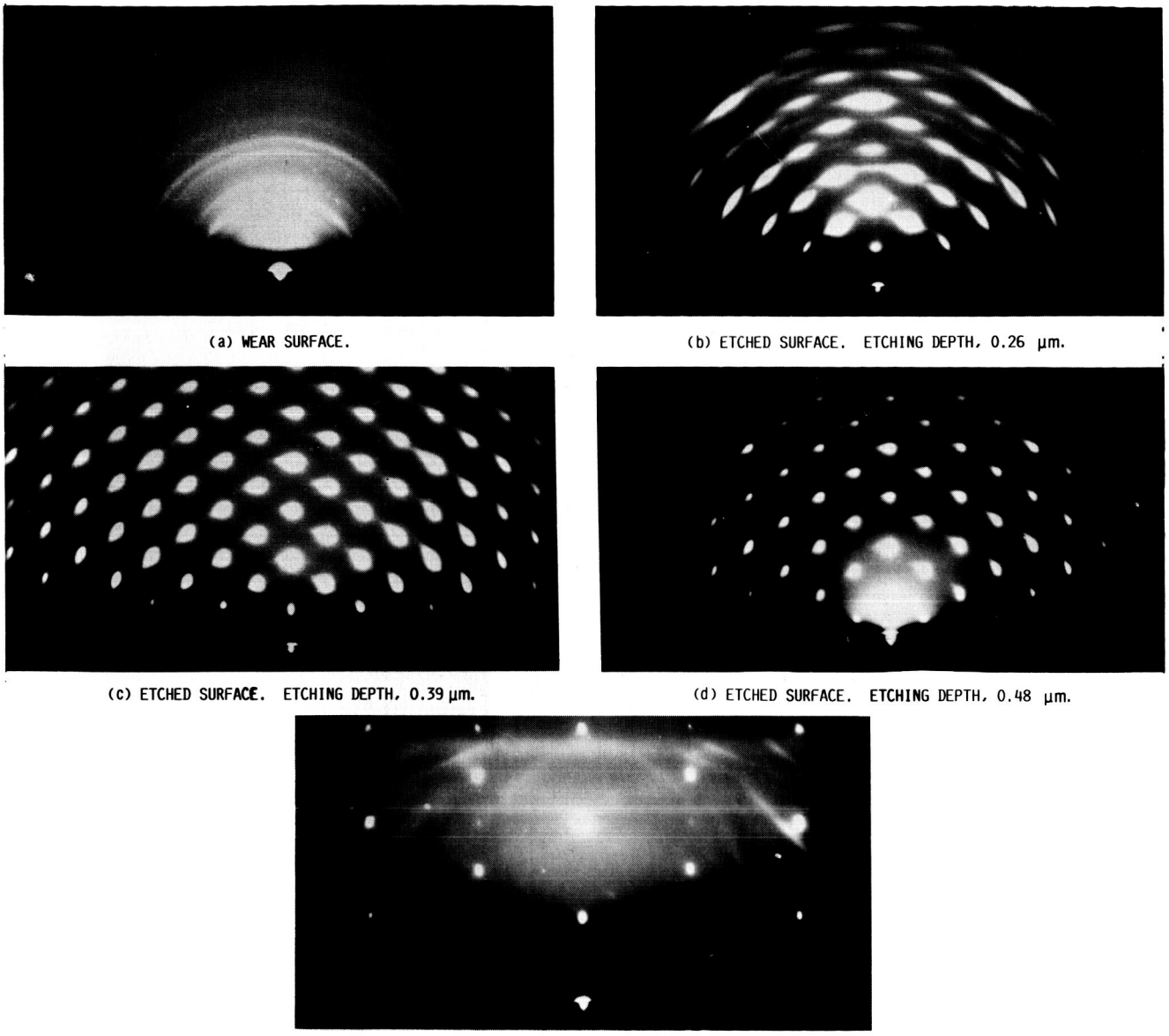

(a) WEAR SURFACE.

(b) ETCHED SURFACE. ETCHING DEPTH, 0.26 μm.

(c) ETCHED SURFACE. ETCHING DEPTH, 0.39 μm.

(d) ETCHED SURFACE. ETCHING DEPTH, 0.48 μm.

(e) ETCHED SURFACE. ETCHING DEPTH, 1.1 μm.

FIGURE 8. - DEFORMED LAYER OF SINGLE-CRYSTAL {100} SURFACE OF Mn-Zn FERRITE ABRADED BY 2-μm (6000-MESH) SiC GRITS. APPARENT CONTACT PRESSURE, 4 N/cm^2; SLIDING DIRECTION, <011>.

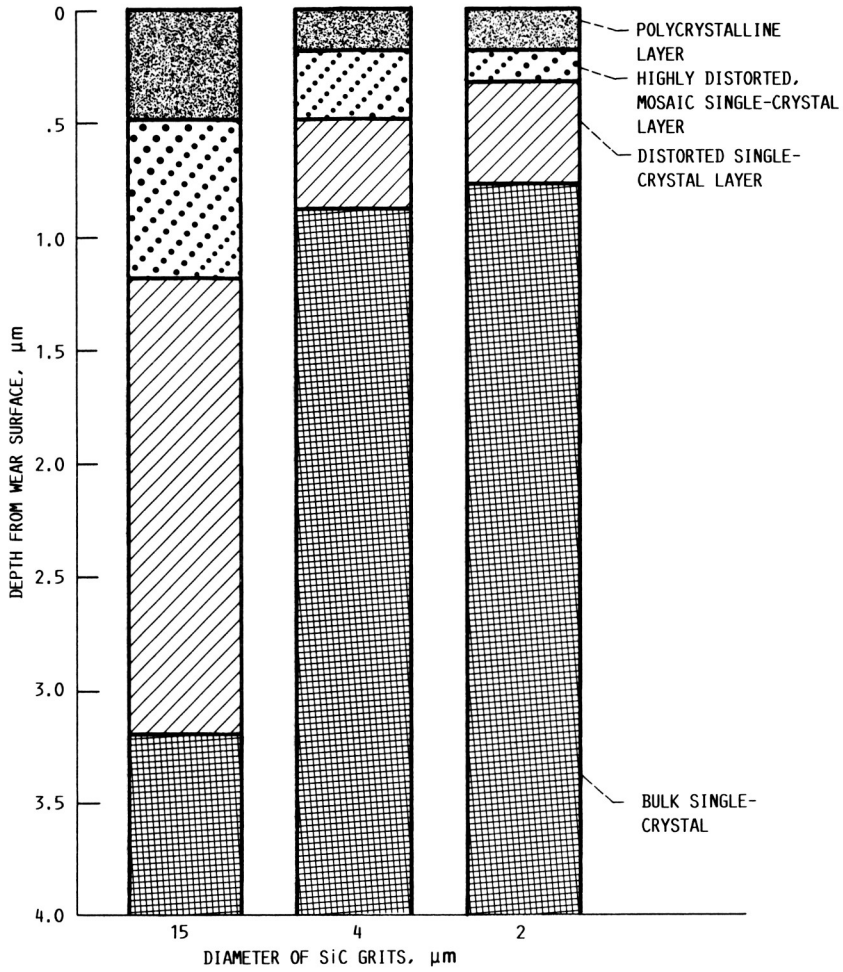

FIGURE 9. - DEFORMED LAYER PRODUCED ON SINGLE-CRYSTAL {100} SURFACE OF Mn-Zn FERRITES AS FUNCTION OF ABRASIVE GRIT SIZE UNDER THREE-BODY ABRASION. APPARENT CONTACT PRESSURE, 4 N/cm^2; SLIDING DIRECTION, $\langle 0\bar{1}1 \rangle$.

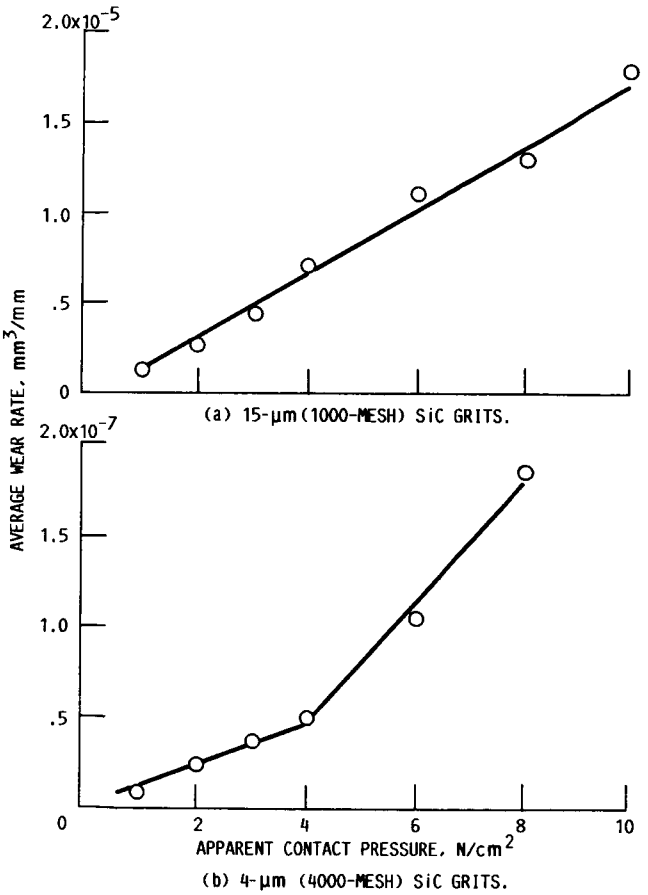

FIGURE 10. - WEAR OF SINGLE-CRYSTAL Mn-Zn FERRITE ABRADED BY SiC GRITS IN THREE-BODY CONDITION.

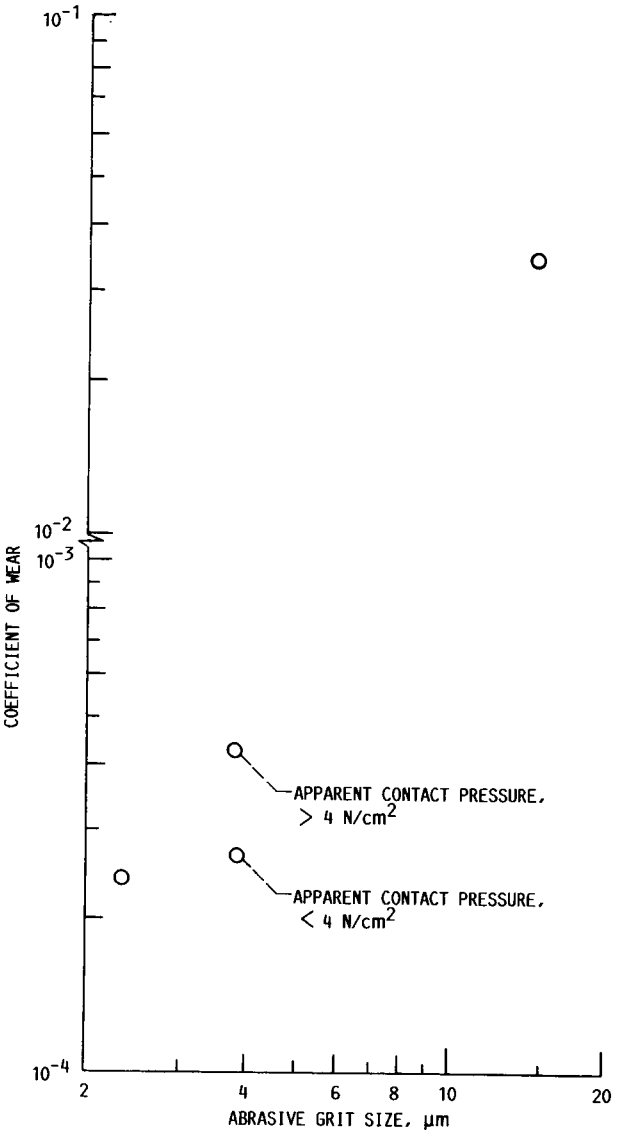

FIGURE 11. - COEFFICIENT OF WEAR FOR SINGLE-CRYSTAL Mn-Zn FERRITE UNDER THREE-BODY ABRASION AS A FUNCTION OF ABRASIVE GRIT SIZE.

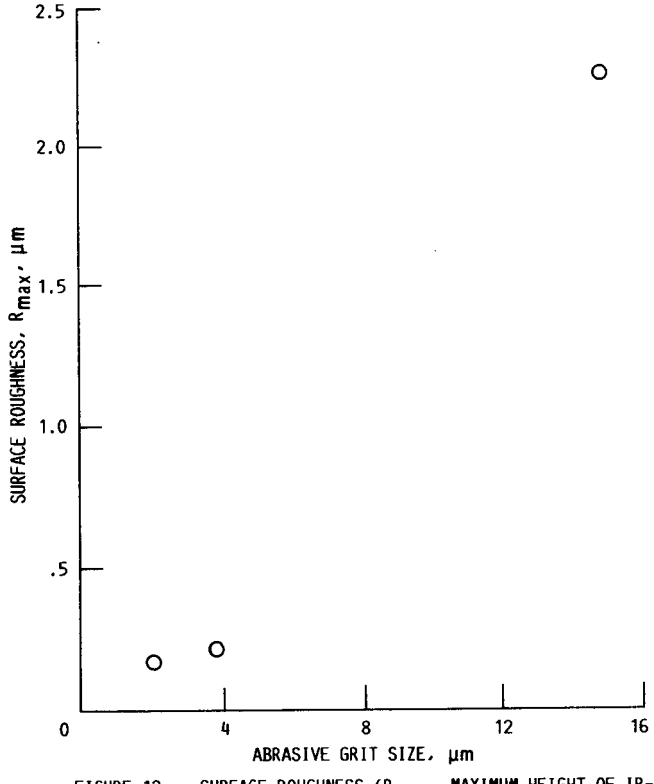

FIGURE 12. - SURFACE ROUGHNESS (R_{max}, MAXIMUM HEIGHT OF IRREGULARITIES) OF SINGLE-CRYSTAL Mn-Zn FERRITE AS FUNCTION OF ABRASIVE GRIT SIZE. APPARENT CONTACT PRESSURE, 4 N/cm^2.

1. Report No.	2. Government Accession No.	3. Recipient's Catalog No.
NASA TM-89879		

4. Title and Subtitle	5. Report Date
Effect of Abrasive Grit Size on Wear of Manganese-Zinc Ferrite Under Three-Body Abrasion	6. Performing Organization Code: 506-43-11
7. Author(s): Kazuhisa Miyoshi	8. Performing Organization Report No.: E-3559
	10. Work Unit No.
9. Performing Organization Name and Address: National Aeronautics and Space Administration, Lewis Research Center, Cleveland, Ohio 44135	11. Contract or Grant No.
	13. Type of Report and Period Covered: Technical Memorandum
12. Sponsoring Agency Name and Address: National Aeronautics and Space Administration, Washington, D.C. 20546	14. Sponsoring Agency Code

15. Supplementary Notes

Prepared for the 1987 Joint Tribology Conference cosponsored by the American Society of Lubrication Engineers and the American Society of Mechanical Engineers, San Antonio, Texas, October 5-8, 1987.

16. Abstract

Wear experiments were conducted using replication electron microscopy and reflection electron diffraction to study abrasion and deformed layers produced in single-crystal Mn-Zn ferrites under three-body abrasion. The abrasion mechanism of Mn-Zn ferrite changes drastically with the size of abrasive grits. With 15-μm (1000-mesh) SiC grits, abrasion of Mn-Zn ferrite is due principally to brittle fracture; while with 4- and 2-μm (4000- and 6000-mesh) SiC grits, abrasion is due to plastic deformation and fracture. Both microcracking and plastic flow produce polycrystalline states on the wear surfaces of single-crystal Mn-Zn ferrites. Coefficient of wear, total thickness of the deformed layers, and surface roughness of the wear surfaces increase markedly with an increase in abrasive grit size. The total thicknesses of the deformed layers are 3 μm for the ferrite abraded by 15-μm SiC, 0.9 μm for the ferrite abraded by 4-μm SiC, and 0.8 μm for the ferrite abraded by 1-μm SiC.

17. Key Words (Suggested by Author(s))	18. Distribution Statement
Abrasive wear Mn-Zn ferrite	Unclassified - unlimited STAR Category 27

19. Security Classif. (of this report)	20. Security Classif. (of this page)	21. No. of pages	22. Price*
Unclassified	Unclassified	25	A02

*For sale by the National Technical Information Service, Springfield, Virginia 22161